Rab-coupling protein coordinates recycling of α5β1 integrin and EGFR1 to promote cell migration in 3D microenvironments

Patrick T. Caswell,[1] May Chan,[2] Andrew J. Lindsay,[3] Mary W. McCaffrey,[3] David Boettiger,[2] and Jim C. Norman[1]

[1]Beatson Institute for Cancer Research, Bearsden, Glasgow G61 1BD, Scotland, UK
[2]Department of Microbiology, University of Pennsylvania, Philadelphia, PA 19104
[3]Molecular Cell Biology Laboratory, Biochemistry Department, Biosciences Institute, University College Cork, Cork, Republic of Ireland

Here we show that blocking the adhesive function of αvβ3 integrin with soluble RGD ligands, such as osteopontin or cilengitide, promoted association of Rab-coupling protein (RCP) with α5β1 integrin and drove RCP-dependent recycling of α5β1 to the plasma membrane and its mobilization to dynamic ruffling protrusions at the cell front. These RCP-driven changes in α5β1 trafficking led to acquisition of rapid/random movement on two-dimensional substrates and to a marked increase in fibronectin-dependent migration of tumor cells into three-dimensional matrices. Recycling of α5β1 integrin did not affect its regulation or ability to form adhesive bonds with substrate fibronectin. Instead, α5β1 controlled the association of EGFR1 with RCP to promote the coordinate recycling of these two receptors. This modified signaling downstream of EGFR1 to increase its autophosphorylation and activation of the proinvasive kinase PKB/Akt. We conclude that RCP provides a scaffold that promotes the physical association and coordinate trafficking of α5β1 and EGFR1 and that this drives migration of tumor cells into three-dimensional matrices.

Introduction

Cell migration is essential to processes such as embryonic development and wound healing but also drives the pathology of diseases such as cancer. Indeed, one of the features of malignant cells, and one that makes cancer so difficult to treat, is their capacity to migrate invasively through the stroma to form metastases (Sahai, 2005). Cell migration can be random or persistent. In 2D, on stiff substrates, cells tend to adopt a polar form with a leading lamellipodium, whereas in 3D they can assume elongated or amoeboid morphologies (Sahai, 2005). A cell's ability to switch between these migrational modes is likely dictated by the way in which it interacts with and responds to the surrounding ECM. Integrins are heterodimeric transmembrane receptors that physically link the ECM to the intracellular actin cytoskeleton but are also signaling molecules that transduce signals bidirectionally across the plasma membrane (Hynes, 2002). The signaling capacity of certain integrin heterodimers has been linked with particular modes of cell migration. For example, a study on epithelial cells has concluded that activation of Rac downstream of αvβ3 integrin promotes slow/persistent migration, whereas engagement of α5β1 that acts via RhoA-ROCK signaling drives rapid/random cell movement (Danen et al., 2005).

Osteopontin is a secreted matrix molecule that becomes incorporated into mineralized bone matrix and a ligand for several cell surface receptors including CD44 and αvβ3 integrin (Rangaswami et al., 2006). Increased secretion of osteopontin is associated with a range of malignancies and correlates strongly with tumor progression and metastasis (Rittling and Chambers, 2004; Khodavirdi et al., 2006). Some tumors secrete large quantities of soluble osteopontin, which does not become incorporated into immobile ECM and is, therefore, unlikely to mediate adhesive interactions between cells and the matrix (Rittling et al., 2002). Nevertheless, osteopontin promotes chemotactic cell migration of several cancer cell lines (Tuck et al., 1999).

Correspondence to Jim Norman: j.norman@beatson.gla.ac.uk

Abbreviations used in this paper: FIP, family of interacting protein; FN, fibronectin; RBD, Rab11-binding domain; RCP, Rab-coupling protein; Rip11, Rab11-interacting protein; RTK, receptor tyrosine kinase; shRNA, short hairpin RNA; Tfn-R, transferrin receptor.

The online version of this article contains supplemental material.

The Rockefeller University Press $30.00
J. Cell Biol. Vol. 183 No. 1 143–155
www.jcb.org/cgi/doi/10.1083/jcb.200804140

Although it has been shown that osteopontin-driven migration may involve modulation of EGF receptor and c-Src signaling (Tuck et al., 2003; Das et al., 2004), the relationship between the binding of osteopontin to αv integrins and the acquisition of tumor cell invasive capacity is not known.

Surface integrins are continuously endocytosed, and then efficiently returned (or recycled) back to the plasma membrane (Caswell and Norman, 2006; Jones et al., 2006; Pellinen and Ivaska, 2006). The way in which integrins are recycled dictates the migrational mode of fibroblasts, and this is largely owing to the influence of recycling pathways on α5β1 (White et al., 2007). Small GTPases of the Rab11 family, including Rab11a and Rab25, control recycling of internalized α5β1 (Roberts et al., 2001; Caswell et al., 2007), and this is likely to require the contribution of at least one Rab11 effector protein. The Rab11 family of interacting proteins (Rab11-FIPs) bind to GTP-bound Rab11s and have been shown to be effectors of Rab11 (Hales et al., 2001; Lindsay et al., 2002; Lindsay and McCaffrey, 2002; Wallace et al., 2002; Prekeris, 2003; Peden et al., 2004; Horgan et al., 2007), thus making them potential candidates for components of protein complexes that control α5β1 recycling. The Rab11-FIPs share a highly homologous C-terminal Rab11-binding domain (RBD) and are categorized into two subfamilies according to their domain structures (Wallace et al., 2002; Prekeris, 2003). The three identified class I FIPs (Rab-coupling protein [RCP; aka Rab11-FIP1], Rab11-FIP2, and Rab11-interacting protein [Rip11; aka pp75 and Rab11-FIP5]) possess an N-terminal phosphatidic acid/phosphatidylinositol 3,4,5-trisphosphate–binding C2 domain (Lindsay and McCaffrey, 2004a), whereas the two class II FIPs (Rab11-FIP3 and Rab11-FIP4) can bind to Arf6 as well as Rab11s and are thus considered to be effectors for both these classes of GTPase (Hickson et al., 2003; Horgan et al., 2004). It is now becoming clear that Rab11-regulated processes can be linked to cancer (Goldenring et al., 1999). Indeed, Rab25 contributes to the aggressiveness of breast and ovarian cancers (Cheng et al., 2004) and likely achieves this in part by altering the trafficking of α5β1 to promote invasive migration (Caswell et al., 2007). Furthermore, Rab11 controls recycling of α6β4 integrin in breast cancer cells in a way that may contribute to hypoxia-induced invasive migration (Yoon et al., 2005). These findings, in combination with the fact that the gene for RCP is located within a small amplicon (8p11-12) prevalent in breast cancer (Gelsi-Boyer et al., 2005), led us to investigate a potential role for class I Rab11-FIPs in coordinating the trafficking of integrins and other proinvasive receptors as tumor cells migrate in 3D microenvironments in response to tumor-relevant chemokinetic factors such as osteopontin and EGF.

Results

Inhibition of αvβ3 promotes α5β1 recycling in A2780 cells

We have previously shown that perturbation of "short-loop" αvβ3 recycling leads to a marked increase in α5β1 recycling (White et al., 2007), so we sought to determine whether such reciprocative cross talk between these two integrins also occurs in cancer cells. The basal recycling rate of α5β1 integrin A2780 ovarian cancer cells was similar to fibroblasts, with 25–30% of internalized integrin returned to the plasma membrane within 15 min (Fig. 1 A, left). However, in cells challenged with either cilengitide (a cyclic RGD peptide known to bind to and inhibit αvβ3 and αvβ5), cRGDfV (a cyclic peptide with selectivity for αvβ3 over αvβ5 integrin; Dechantsreiter et al., 1999), or the soluble αvβ3 ligand osteopontin, α5β1 recycling increased by at least twofold, whereas a control cyclic peptide (cRADfV) was ineffective in this regard (Fig. 1 A, left). Consistent with this, suppression of β3 levels by RNAi (Fig. S1, available at available at http://www.jcb.org/cgi/content/full/jcb.200804140/DC1) increased α5β1 recycling, and treatment of β3 knockdown cells with either cilengitide or osteopontin did not further enhance α5β1 trafficking (Fig. 1 A, right). Cilengitide did not affect the rate at which α5β1 was internalized by A2780 cells (Fig. S1 B). As cilengitide-driven α5β1 recycling was Rab11 dependent (Fig. S2 A), these data indicate that αvβ3 functions constitutively to restrain α5β1 recycling in A2780 ovarian cancer cells and that removal of αvβ3 or its occupation/blockade with soluble, non-ECM ligands such as osteopontin or cilengitide releases this constraint to drive Rab11-dependent trafficking of α5β1 to the plasma membrane.

Inhibition of αvβ3 drives α5β1 and RCP into a coprecipitable complex

Because physical associations may be formed between Rab effectors and their cargoes (Fan et al., 2004), we immunoprecipitated members of the class I family of Rab11 effectors from A2780 cells and probed for the presence of α5β1 and αvβ3 integrins. This revealed that RCP associated with both α5β1 and αvβ3 integrins (Fig. 1 B) and pretreatment of the cells with cilengitide (Fig. 1, B and D) or osteopontin (Fig. 1 D) strongly promoted coprecipitation of RCP with α5β1 but reduced its association with αvβ3 (Fig. 1 B). Increased association of α5β1 and RCP was detectable within 8 min and was maximal after 20-min exposure to cilengitide (Fig. S3 A, available at http://www.jcb.org/cgi/content/full/jcb.200804140/DC1). To further confirm these associations, we immunoprecipitated α5β1 and αvβ3 using antibodies recognizing α5 and β3 integrin, respectively. Western blots of these immunoprecipitates indicated that both endogenous and overexpressed RCP coprecipitated with α5β1 and αvβ3 (but not with a control antibody) and that addition of cilengitide strongly promoted RCP's association with α5β1, but correspondingly weakened binding to αvβ3 (Fig. 1 C). Suppression of β3 expression by RNAi also increased association between RCP and α5β1, and treatment of β3 knockdown cells with cilengitide or osteopontin did not further enhance this (Fig. 1 D). Furthermore, RCP^{621E}, containing a point mutation within the RBD of RCP rendering it unable to interact with Rab11 (and therefore to be considered a dominant-negative inhibitor of RCP function), did not associate with α5β1 (Fig. 1 E), indicating that Rab11 likely contributes to α5β1–RCP complex formation.

RCP regulates integrin recycling and α5β1-dependent cell movement

Although cilengitide promoted α5β1 recycling in cells expressing control RNAi or those overexpressing RCP^{wt}, it was completely

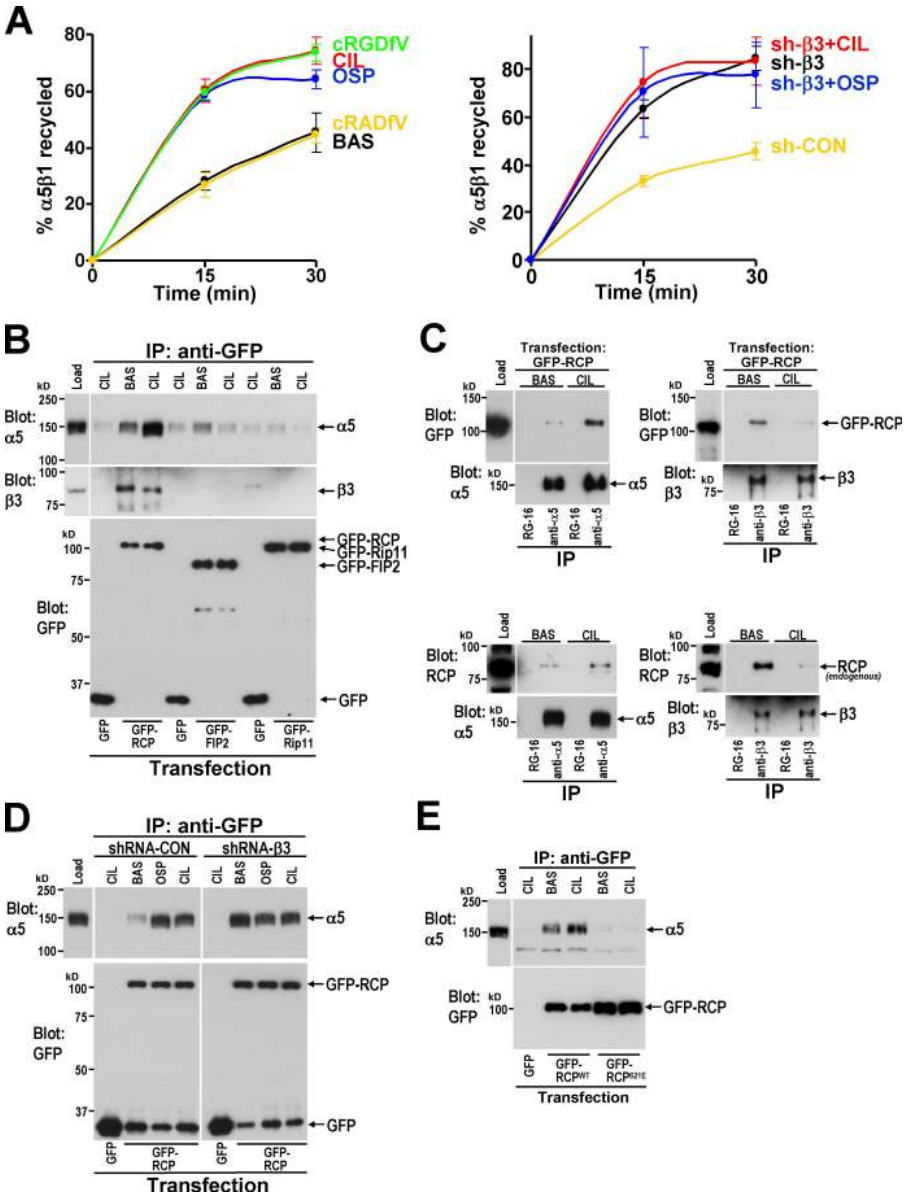

Figure 1. **Inhibition of αvβ3 promotes α5β1 recycling and association of RCP with α5β1.** (A) A2780 cells were transfected with a nontargeting shRNA (sh-CON) or a short hairpin–targeting β3 integrin (sh-β3; right) or were left untransfected (left). Cells were surface labeled with 0.2 mg/ml NHS-S-S-Biotin at 4°C and internalization was then allowed to proceed for 30 min at 37°C. Biotin remaining at the cell surface was removed by exposure to MesNa at 4°C, and internalized integrin was chased back to the cell surface at 37°C for the indicated times in the absence (BAS) or presence (CIL) of 1 μM cilengitide, 1 μM c-RADfV, 4.4 μM cRGDfV, or 0.5 μg/ml soluble osteopontin. Cells were then reexposed to MesNa and biotinylated integrin was determined by capture ELISA using microtitre wells coated with anti-human α5 integrin monoclonal antibodies. The proportion of integrin recycled to the plasma membrane is expressed as a percentage of the pool of integrin labeled during the internalization period. (left) Values are mean ± SEM; $n = 7$ (BAS), $n = 4$ (CIL), and $n = 3$ (cRADfV, cRGDfV, and OSP) independent experiments. (right) Values are mean ± SEM; $n = 3$ independent experiments. (B) A2780 cells were transfected with plasmids encoding GFP or GFP fused to the class I FIPs (GFP-RCP, GFP-FIP2, and GFP-Rip11). Transfected cells were incubated in the absence (BAS) or presence (CIL) of 1 μM cilengitide for 20 min and lysed in a buffer containing 0.15% Tween-20. GFP and GFP fusion proteins were immunoprecipitated from lysates by incubation with beads coupled to a monoclonal antibody recognizing GFP, and these immunoprecipitates analyzed for the presence of α5β1 and αvβ3 by immunoblotting with antibodies recognizing the integrin α5 and β3 chains, respectively. The loading of GFP and GFP fusions was confirmed by immunoblotting with an antibody recognizing GFP (bottom). (C) Cells were transfected with GFP-RCP (top) or left untransfected (bottom), and then incubated in the absence (BAS) or presence (CIL) of 1 μM cilengitide for 20 min. Lysates were immunoprecipitated using monoclonal antibodies recognizing α5β1 integrin (anti-α5), αvβ3 integrin (anti-β3), or an isotype-matched control antibody (RG-16). The presence of α5 and β3 integrin, GFP-RCP, and endogenous RCP were detected by immunoblotting. (D) After cotransfection of GFP or GFP-RCP with either nontargeting shRNA (shRNA-CON) or a short hairpin targeting β3 integrin (shRNA-β3), A2780 cells were incubated in the absence (BAS) or presence (CIL) of 1 μM cilengitide or 0.5 μg/ml osteopontin (OSP) for 20 min. Cells were lysed and anti-GFP immunoprecipitates probed for the presence of α5β1 and GFP as in B. (E) A2780 cells were transfected with GFP, GFP-RCP^{wt}, or GFP-RCP^{621E}, treated with cilengitide, and then lysed. Anti-GFP immunoprecipitates were probed for α5β1 and GFP as in B.

unable to drive α5β1 recycling after RCP knockdown or expression of dominant-negative RCP^{621E} (Fig. 2 A). The corresponding dominant-negative mutants of Rip11 or Rab11-FIP2 (Rip11^{630E} and FIP2^{481E}) had no effect on cilengitide-induced α5β1 recycling (Fig. S2 B), and RCP^{621E} did not compromise trafficking of the transferrin receptor (Tfn-R) in the presence or absence of cilengitide (Fig. S2 C). Internalization of α5β1 was not affected by expression of dominant-negative RCP (Fig. S1 B). These data indicate that RCP displays selectivity toward the recycling of specific cargoes (i.e., α5β1 not Tfn-R) that follow Rab11-dependent routes to the cell surface and that RCP is likely to be the only class I FIP that has a role in trafficking α5β1.

As increased α5β1 recycling causes fibroblasts to switch from persistent to random migration (White et al., 2007), we analyzed the movement of A2780 cells as they migrated into scratch wounds. A2780 cells migrated persistently after wounding (Video 1, available at http://www.jcb.org/cgi/content/full/jcb.200804140/DC1), but treatment with either cilengitide (Video 2) or osteopontin induced a significantly more rapid but less persistent mode of migration, and α5β1 was required for the increase in speed (Fig. 2 B). In the absence of cilengitide, expression of RCP^{621E} did not effect cell migration. However, RCP^{621E} (but not dominant-negative Rab11-FIP2 or Rip11) completely opposed the cilengitide- or osteopontin-driven increase in migration speed (Fig. 2 B), such that in the combined presence of the cyclic peptide and dominant-negative RCP the cells appeared to wobble on the spot and were largely unable to move away from their original positions (Video 3).

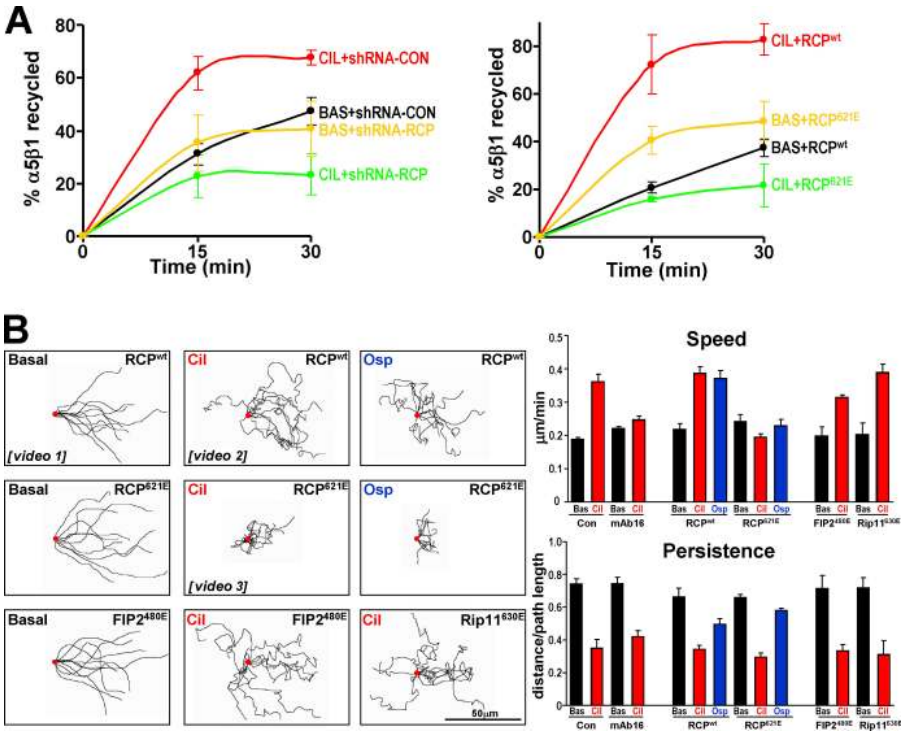

Figure 2. **Cilengitide and osteopontin drive alterations in α5β1 recycling and cell migration that are dependent on RCP.** (A) A2780 cells were transfected with a nontargeting shRNA (shRNA-CON), a short hairpin targeting RCP (shRNA-RCP), GFP-RCP^{wt}, or dominant-negative GFP-RCP^{621E}. Recycling of α5β1 integrin was determined in the presence and absence of 1 μM cilengitide as for Fig. 1 A. Values are mean ± SEM; *n* = 3 independent experiments. (B) Cells were transfected with GFP-RCP^{wt} or GFP-RCP^{621E} and allowed to grow to confluence. Confluent monolayers were wounded with a plastic pipette tip and the cells were allowed to migrate into the wound in the absence (Basal) or presence of 1 μM cilengitide (Cil) or 0.5 μg/ml osteopontin (Osp). The cells were observed by time-lapse video microscopy, the movement of individual cells followed using cell tracking software, and this is presented as overlays of representative trajectories described by cells during the first 9 h of their migration into the wound. The starting position of each cell is denoted by the red dot. Examples of time-lapse movies that correspond to these experiments are included as Videos 1–3 as indicated (available at http://www.jcb.org/cgi/content/full/jcb.200804140/DC1). The persistence and speed of migration were extracted from the track plots. Persistence is defined as the ratio of the vectorial distance traveled to the total path length described by the cell. Values are mean ± SEM; *n* = 3 independent experiments. Bar, 50 μm.

Fluorescence time-lapse imaging revealed that migrating A2780 cells adopted a fanlike morphology in which the actin-rich lamellipodium advanced in an organized, processive fashion, with retrograde movement of filaments back from the leading edge being clearly visible (Video 4, available at http://www.jcb.org/cgi/content/full/jcb.200804140/DC1). Furthermore, 3D reconstruction of serial z stack confocal images indicated that the F-actin–rich lamellipodial tip of migrating A2780 cells did not rise much above the surface of the substratum (Fig. 3 A, left). However, upon challenge with cilengitide or osteopontin, or when αvβ3 was suppressed by RNAi, the morphology of migrating A2780 cells was drastically altered, with an apparent collapse of the lamellipodium and the presence of anterior protrusions containing α5β1 integrin, RCP, and F-actin (Fig. S4). 3D reconstructions indicated that these protrusions were composed of numerous actin-rich ruffles that extended upward from the cell front (Fig. 3 A, middle and right). Fluorescence time-lapse imaging showed these cilengitide- and osteopontin-driven structures to be very actively protrusive and always anterior to the direction of migration (Videos 4–6), indicating that they were neither dorsal ruffles nor retracting lamellae, but likely locomoting structures contributing to the cell's forward motion. Moreover, expression of dominant-negative RCP (but not dominant-negative FIP2 or Rip11) blocked the ability of A2780 cells to extend these anterior ruffling protrusions (Fig. 3 B), indicating a requirement for RCP (but not other class I Rab11-FIPs) in this type of cell migration.

RCP and α5β1 promote fibronectin (FN)-dependent migration in 3D

The capacity of α5β1 to support migration in 3D matrices is dictated by the way in which it is trafficked. Indeed, α5β1 and FN inhibit invasive migration of Fos-transformed fibroblasts through matrigel (Spence et al., 2006). However, expression of Rab25 changes the way in which α5β1 is trafficked such that α5β1 supports migration of Fos-transformed fibroblasts through 3D FN-containing matrices (Caswell et al., 2007). We, therefore, sought to determine whether cilengitide-driven, RCP-dependent changes in α5β1 trafficking were sufficient to promote migration into 3D matrices. When αvβ3 was not inhibited, migration of A2780 cells was unaffected by addition of FN to the matrigel (Fig. 4 A). However, addition of cilengitide or osteopontin strongly promoted FN-dependent migration of A2780 cells into matrigel plugs (Fig. 4 A). Experiments using blocking antibodies and RNAi of integrin subunits indicated that this component of migration was dependent on the presence and RGD ligand–binding capacity of α5β1 integrin (Fig. 4 B). Depletion of β3 integrin with RNAi strongly promoted FN-dependent migration into matrigel (in the absence of FN, β3 knockdown suppressed migration), and neither cilengitide nor osteopontin were able to further increase this (Fig. 4 A). Although basal migration of A2780 cells did not require RCP, the cilengitide-driven increase in migration through matrigel was suppressed by dominant-negative RCP^{621E} or short hairpin RNA (shRNA) of RCP (Fig. 4 C), but was not affected by the corresponding mutants of Rab11-FIP2 or Rip11 (Fig. S5 A, available at http://www.jcb.org/cgi/content/full/jcb.200804140/DC1).

To determine how cilengitide promotes cell migration in 3D, while minimizing the technical difficulties in imaging cell migration within dense 3D microenvironments, we analyzed the migration of cells plated onto cell-derived matrix. We have previously found that expression of Rab25 induced A2780 cells to be more invasive and to switch their mode of migration to one that is

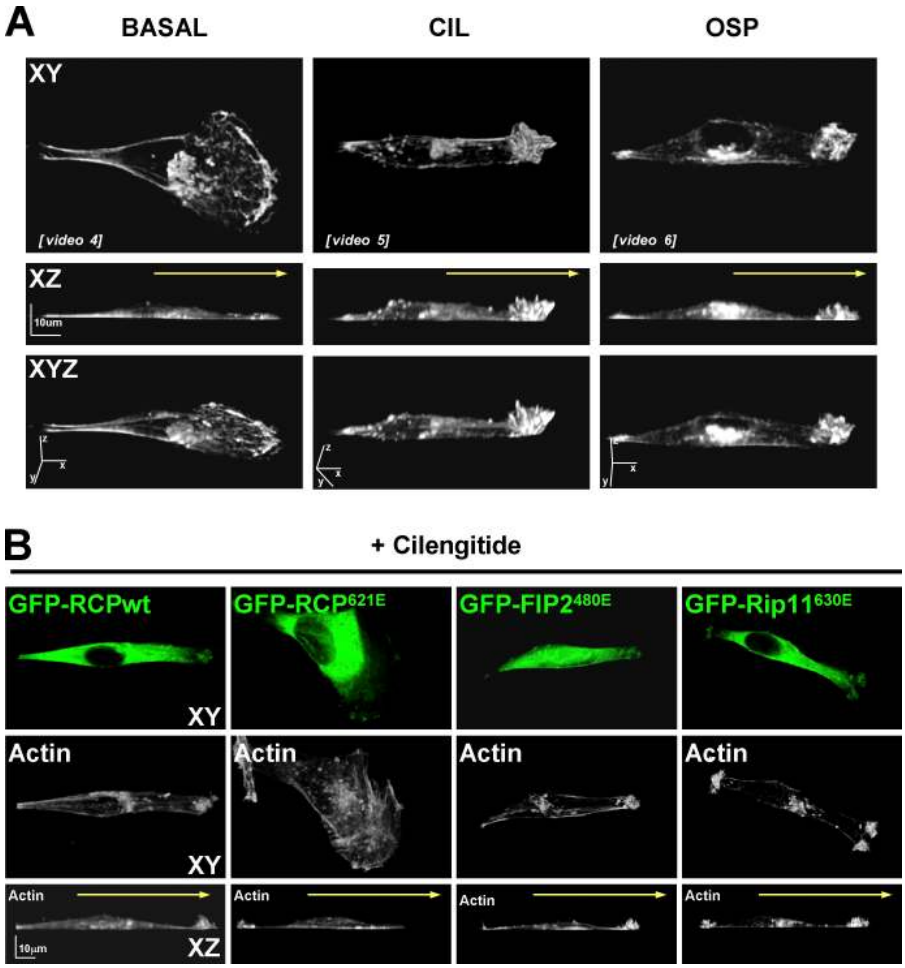

Figure 3. **Inhibition of αvβ3 promotes the formation of dynamic actin-rich protrusions at the cell front.** (A) Confluent monolayers were wounded with a plastic pipette tip and the were cells allowed to migrate for 2 h into the wound in the absence (BASAL) or presence of 1 μM cilengitide (CIL) or 0.5 μg/ml osteopontin (OSP). Cells were fixed and permeabilized and F-actin was visualized using fluorescently conjugated phalloidin. 3D reconstructions were generated from serial Z sections captured using a confocal microscope. Yellow arrow denotes the direction of cell migration. Bar, 10 μm. Time-lapse movies indicating the dynamics of GFP-actin under conditions corresponding to the experiments presented in A are included as Videos 4–6, respectively (available at http://www.jcb.org/cgi/content/full/jcb.200804140/DC1). (B) A2780 cells were transfected with GFP-RCP^{wt}, GFP-RCP^{621E}, GFP-FIP2^{480E}, or GFP-Rip11^{630E}. Confluent monolayers were wounded with a plastic pipette tip and the cells were allowed to migrate for 2 h into the wound in the absence or presence of 1 μM cilengitide. Cells were fixed and permeabilized and GFP and F-actin was visualized by fluorescence microscopy. 3D reconstructions were generated from serial Z sections captured using a confocal microscope. Yellow arrow denotes the direction of cell migration. Bar, 10 μm.

characterized by the extension of long pseudopods (Caswell et al., 2007). As previously observed, A2780 cells migrated rapidly across cell-derived matrices and maintained their overall sluglike morphology as they moved (Fig. 5 A and Video 7, available at http://www.jcb.org/cgi/content/full/jcb.200804140/DC1). Addition of cilengitide altered the morphology of cells migrating on 3D matrices to extend long pseudopods in the direction of migration (Fig. 5, A and B; and Video 8). When αvβ3 was not inhibited, migration on cell-derived matrix had no requirement for RCP (Fig. 5 A), but expression of RCP^{621E} completely abrogated cilengitide-driven pseudopodial extension and markedly decreased both the speed and persistence of cell movement (Fig. 5, A and B; and Video 9). The dynamic localization of RCP within migrating cells was also strikingly altered by treatment with cilengitide. In untreated cells, GFP-RCP localized to the perinuclear region and to vesicles distributed fairly uniformly throughout the cytoplasm (Fig. 5 C). However, after addition of cilengitide, GFP-RCP (but not dominant-negative GFP-RCP^{621E}) was recruited to the tip of the extending pseudopod (Fig. 5 C). Although there was considerable movement of RCP-positive tubulovesicular structures in and out of the pseudopodial region, the RCP-containing structures at the distal pseudopod tip appeared to be relatively immobile and closely associated with the plasma membrane. Collectively, these data indicate that inhibition of αvβ3 strongly promotes RCP-dependent trafficking of α5β1 integrin, which alters cellular morphology to favor rapid/random movement on plastic surfaces and a pseudopodial-driven mode of migration on a 3D matrix.

RCP-regulated recycling does not affect the ability of α5β1 to bind to FN

Regulation of integrin internalization and recycling may influence cell adhesion and migration by controlling the level of heterodimer exposed at the plasma membrane. Addition of cilengitide and expression of mutant RCPs influence the amount of α5β1 expressed at the cell surface (Fig. S5 B), but do so only modestly and to a degree that is consistent with the way that they alter recycling from a relatively small (~15–20% of the quantity of surface receptor [not depicted]) intracellular pool of α5β1 integrin. We had, therefore, previously hypothesized that endosomal pathways may not function primarily to control the quantity of surface receptors, but that they regulate integrin function in other ways, for example, by "cleaning" internalized integrins of bound ligand, thus maintaining ligand-binding competency (Caswell and Norman, 2006; White et al., 2007). To analyze the effect of recycling on integrin function we used a spinning disc approach, which measures the mean shear stress (τ_{50}) required for cell detachment (Garcia et al., 1998). Because τ_{50} is proportional to the number of α5β1 and αvβ3 integrins per cell that are occupied in adhesive bonds, this provides a direct measure of integrin adhesive

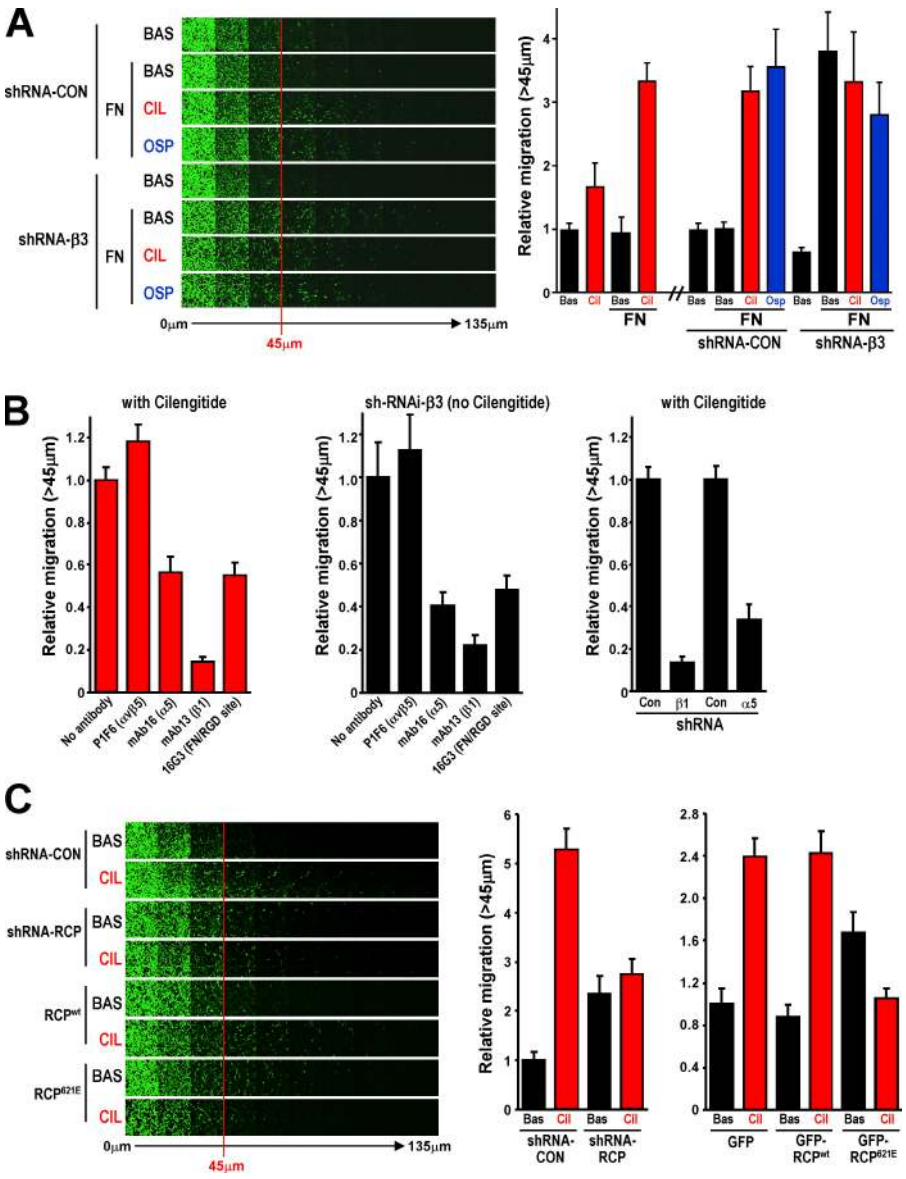

Figure 4. **Inhibition of αvβ3 promotes migration into matrigel that is dependent on RCP and engagement of α5β1 with FN.** (A) Migration of A2780 cells expressing a nontargeting shRNA (shRNA-Con) or a short hairpin targeting β3 integrin (shRNA-β3) into a matrigel plug in the presence and absence of 25 μg/ml FN was determined using an inverted matrigel plug assay. 1 μM cilengitide (CIL) and 0.5 μg/ml osteopontin (OSP) were added as indicated to the matrigel and to both the upper and lower chambers of the inverted matrigel plug assay. Invading cells were stained with Calcein AM and visualized by confocal microscopy. Serial optical sections were captured at 15-μm intervals and are presented as a sequence in which the individual optical sections are placed alongside one another with increasing depth from left to right as indicated. Migration was quantitated by measuring the fluorescence intensity of cells penetrating the matrigel to depths of 45 μm and greater and expressing this as a percentage of the total fluorescence intensity of all cells within the plug. Data represents mean ± SEM from three independent experiments. (B) The involvement of α5β1 integrin in migration driven by addition of cilengitide (left and right) or induced by suppression of αvβ3 levels (middle) was determined by addition of the indicated integrin- and FN-blocking antibodies (left and middle) and also by RNAi of the α5 and β1 subunits of α5β1 (right). Migration was quantified as for A. Values are mean ± SEM from three independent experiments. (C) The migration of A2780 cells expressing nontargeting shRNA (shRNA-CON), a short hairpin targeting RCP integrin (shRNA-RCP), GFP, GFP-RCP^{wt}, or GFP-RCP^{621E} into FN-containing matrigel was determined and quantified as for A.

function (Boettiger et al., 2001; Shi and Boettiger, 2003; Boettiger, 2007). The generation of τ_{50} from curve fits of the spinning data (Fig. 6 A) was used to generate a comparison of integrin bond levels (Fig. 6 B). Addition of cilengitide reduced the total adhesion, as measured by the spinning disc, by ~14% consistent with the contribution that is typically made to adhesion by αvβ3 in cells expressing both αvβ3 and α5β1. As shown in Fig. 3 A, inhibition of RCP reduces cilengitide-driven α5β1 recycling by at least threefold. Therefore, if recycling were to influence α5β1's ligand-binding capacity, one would anticipate a large alteration in adhesion strength after inhibition of RCP. However, expression of RCP^{621E} effected only a small change (10–15% reduction) in adhesion strength (Fig. 6 B), indicating that the quantity and strength of integrin–ligand adhesive bonds is proportional to the level of surface expression (Fig. S5 B) and not to the proportion of integrin recycled. Because RCP does not influence the ligand-binding capacity of α5β1, it is likely that there are alternative explanations for the ability of this type of recycling to promote cell migration and invasiveness.

RCP associates with EGFR1 and α5β1 to coordinate their recycling

As the endosomal pathway is known to have profound influence on the way that many receptors communicate with their downstream effectors (von Zastrow and Sorkin, 2007), it is possible that integrin recycling alters cell migration by influencing the assembly of signalosomes that mediate receptor tyrosine kinase (RTK) signaling. To investigate this possibility we probed RCP immunoprecipitates with antibodies recognizing phosphotyrosine. Although cytoskeletal phosphotyrosine-containing proteins such as paxillin were not present in RCP immunoprecipitates (Fig. S3 B), we consistently observed a high molecular mass phosphotyrosine-rich band with the approximate molecular mass of EGFR1 (not depicted). Indeed, addition of cilengitide, osteopontin, or RNAi of β3 drove α5β1 and EGFR1 into a coprecipitable complex with endogenous or overexpressed RCP (Fig. 6 C), and this correlated closely with recruitment of EGFR1 to F-actin–rich protrusions at the cell front and its colocalization with RCP at these structures (Fig. 6, D–F). Given this coprecipitation of

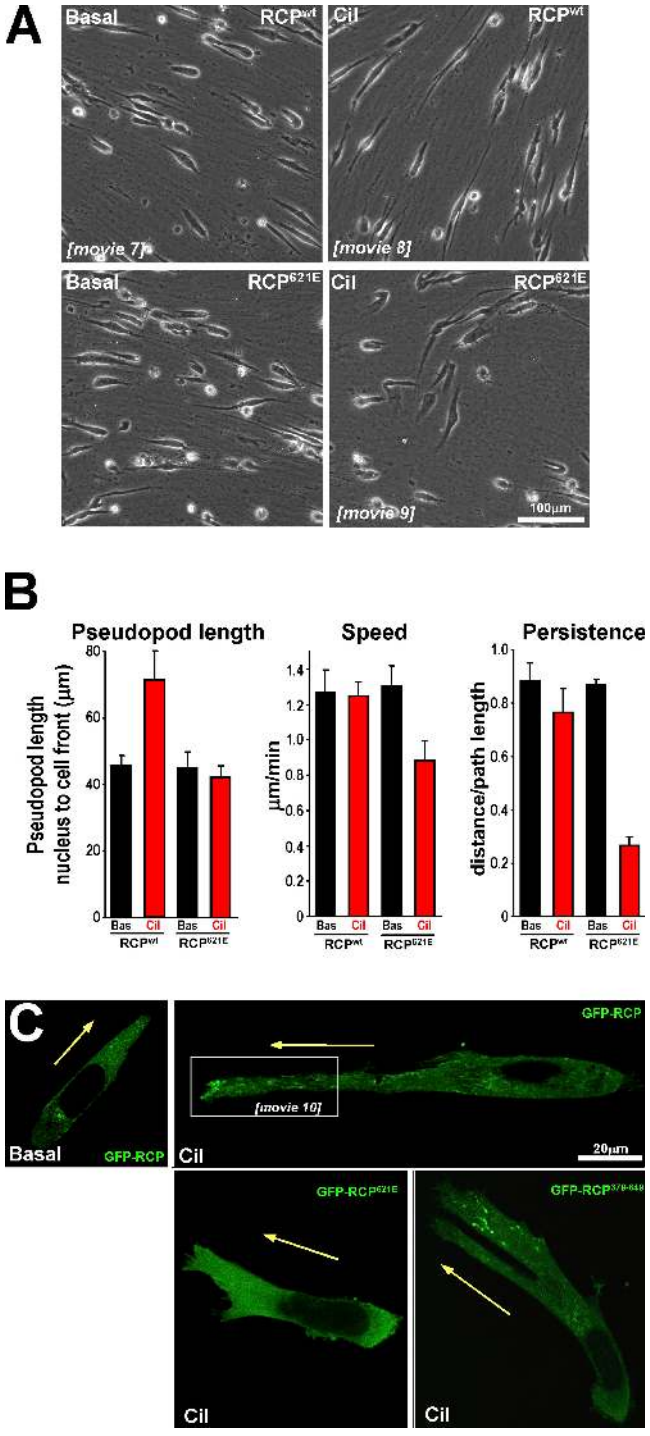

Figure 5. **Cilengitide drives RCP to the tips of extending pseudopods.** (A and B) Cells were transfected with GFP-RCP^{wt} or GFP-RCP^{621E} and plated onto cell-derived matrix in the presence and absence of 1 μM cilengitide ~4 h before time-lapse microscopy. Images were captured every 5 min over a 6-h period and movies were generated from these (Videos 7–9) and stills from these movies are presented. Bar, 100 μm. (B) Speed and persistence of migration were determined as for Fig. 3 B, values are mean ± SEM; *n* = 3 independent experiments. To obtain a measure of pseudopod length, the distance between the center of the nucleus and the cell front (with respect to the direction of migration) was measured using ImageJ. Data represents mean ± SEM; *n* = 3 independent experiments. (C) Cells were transfected with GFP-RCP, GFP-RCP^{621E}, or GFP-RCP$^{379-649}$ and plated onto cell-derived matrix in the presence and absence of 1 μM cilengitide and imaged by confocal microscopy. Images were captured at 1 frame/second over a period of 100 s and movies were generated from these. Single section confocal image stills corresponding to individual frames from these movies are presented. Bar, 20 μm. The yellow arrows indicate the direction of migration and the portion of the cell within the white square is presented as Video 10. Videos are available at http://www.jcb.org/cgi/content/full/jcb.200804140/DC1.

α5β1 with RCP and EGFR1, we sought to determine whether RCP was acting as a molecular bridge to connect α5β1 and EGFR1. First, we found that α5-RNAi prevented coprecipitation of EGFR1 with RCP, whereas EGFR1-RNAi did not reduce association of RCP with α5β1 (Fig. 6 C). Second, we deployed the mutant RCP$^{379-649}$ that lacks an N-terminal portion of the protein, including the C2 domain, but retains the C terminus and Rab11-binding domain. Interestingly, this truncated RCP associated with α5β1 integrin but had no capacity to coprecipitate with EGFR1 (Fig. 6 C). Furthermore, dominant-negative RCP^{621E} did not coprecipitate with either α5 or EGFR1 (Fig. 6 C) and RNAi of RCP prevented coprecipitation of EGFR1 with α5β1 (not depicted). Collectively, these data indicate that the C terminus of RCP interacts with α5β1 to permit an association between the N terminus of RCP with EGFR1, thus bringing these two receptors together into a coprecipitable complex.

The presence of such a physical association between α5β1, RCP, and EGFR1 prompted us to investigate the role of RCP in coordination of α5β1 and EGFR1 trafficking. Cilengitide, osteopontin, cRGDfV, and β3-RNAi promoted EGFR1 recycling to a similar extent as was previously observed for α5β1, and knockdown of RCP prevented this (Fig. 7 A). Furthermore, addition of cilengitide and/or expression of dominant-negative RCP did not affect internalization of EGFR1 by A2780 cells (Fig. S1 B). Suppression of α5 integrin by RNAi blocked the cilengitide-induced increase in EGFR1 recycling, whereas knockdown of EGFR1 had no effect on recycling of α5β1 (Fig. 7 B). Furthermore, expression of RCP$^{379-649}$ (which can associate with α5β1 but not EGFR1) had minimal effect on cilengitide-driven α5β1 recycling, but severely impaired EGFR1 recycling (Fig. 7 C). Collectively, these data indicate that cilengitide-driven recycling of EGFR1 is strongly dependent on α5β1 (but not vice versa) and that effective recycling of EGFR1 requires its association with RCP.

Expression of RCP$^{379-649}$ opposes cilengitide-driven migration into FN-containing matrigel

EGFR1-RNAi inhibited the ability of A2780 cells to migrate into matrigel under all circumstances investigated (unpublished data), indicating a requirement for EGFR1 in the invasive process. To determine the role of trafficking to EGFR1's contribution to migration in 3D, we investigated the consequences of expressing RCP$^{379-649}$ (which has little effect on α5β1 recycling but compromises trafficking of EGFR1) on the ability of cilengitide to drive movement of cells into matrigel. Expression of RCP$^{379-649}$ did not affect the basal migration of A2780 cells but inhibited the ability of cilengitide to drive cells into FN-containing matrix (Fig. 7 D). Moreover, although GFP-RCP$^{379-649}$ was localized to vesicular structures toward the cell front (indicating that integrin binding mediates the recruitment of RCP to extending processes), this

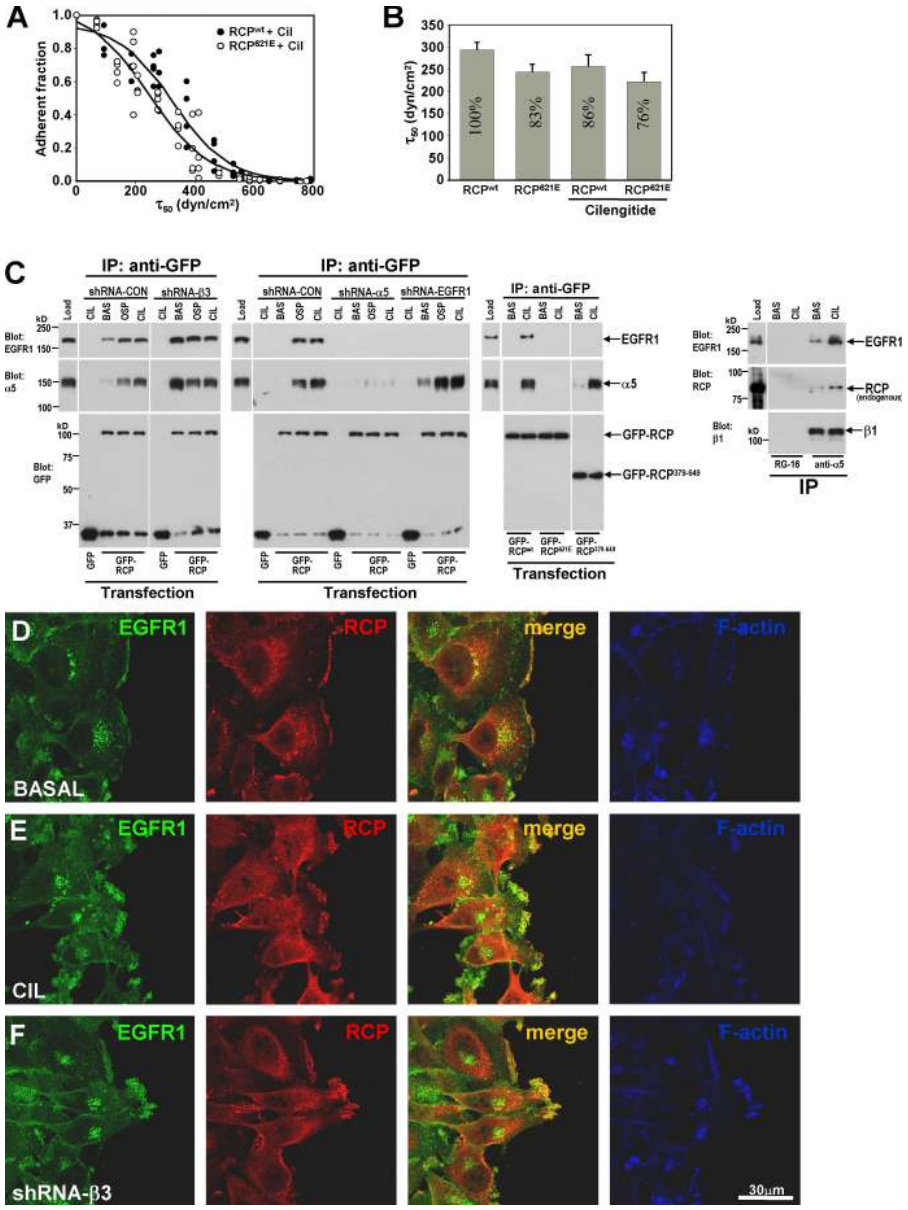

Figure 6. **RCP does not affect integrin ligand-binding ability but mediates an association between α5β1 and EGFR1.** (A and B) A2780 cells were transfected with either RCP^{wt} or the dominant-negative RCP^{621E} and incubated for 24 h ±1 μM cilengitide for the last 16 h. Adhesion to FN was analyzed using the spinning disc. (A) The analysis of cell density at 61 points for each treatment as a function of wall shear stress (τ_{50}) is shown. The associated curve fit (solid lines) R^2 values for the fits are 0.95 (RCP^{wt} with cilengitide) and 0.92 (RCP^{621E} with cilengitide). The curve fits were used to extract a mean shear stress for cell detachment (τ_{50}) that is proportional to the number of adhesive integrin–ligand bonds (Boettiger, 2007). (B) The combined analyses for τ_{50} from three independent experiments run in triplicate are shown; normalized percentages are on the bars. Values are mean ± SEM (n = 8 or 9). (C) Cells were transfected with hairpin vectors targeting β3 integrin, α5 integrin, or EGFR1 in combination with GFP, GFP-RCP^{wt}, or GFP-RCP^{621E} (left), or were left untransfected (right). After incubation with 1 μM cilengitide (CIL) or 0.5 μg/ml osteopontin (OSP), cells were lysed and GFP-RCP or α5β1 was immunoprecipitated from the lysates using monoclonal antibodies recognizing GFP (anti-GFP), α5 integrin (anti-α5), or an isotype-matched control antibody (RG-16). The presence of α5 integrin, GFP-RCP, endogenous RCP, and EGFR1 in the immunoprecipitates was then detected by immunoblotting. (D–F) A2780 cells were transfected with a short hairpin–targeting β3 integrin (shRNA-β3; F) or were left untransfected (D and E). Confluent monolayers were wounded and the cells were allowed to migrate into the wound in the absence (D and F) or presence (E) of 1 μM cilengitide. The distribution of EGFR1 (green), RCP (red), and F-actin (blue) was visualized by immunofluorescence followed by confocal microscopy. Bar, 30 μm.

truncated RCP caused pseudopod bifurcation, suggesting that combined recruitment of EGFR1 and α5β1 is necessary for maintenance of pseudopodial dominance, which is in turn required for cilengitide-driven migration in 3D (Fig. 5 C).

αvβ3's modulation of EGFR1 signaling proceeds via RCP and α5β1

Cilengitide addition and expression of dominant-negative RCP does not greatly affect the exposure of EGFR1 at the cell surface (Fig. S5 B). However, the way in which receptors are trafficked is now established to modulate the downstream signaling profile of several RTKs (von Zastrow and Sorkin, 2007). Indeed, we found that pretreatment of A2780 cells with osteopontin or cilengitide or β3-RNAi (all of which enhance EGFR1 recycling) strongly potentiated the ability of EGF to drive EGFR1 autophosphorylation (Fig. 8, A and B). Pretreatment of cells with either osteopontin or cilengitide enhanced downstream signals to PKB/Akt but phosphorylation of ERK1/2 remained at basal levels (Fig. 8, A and B). Because osteopontin or cilengitide-driven EGFR1 recycling required α5β1 and the association of EGFR1 with RCP, we investigated the involvement of α5 and RCP in EGFR1 signaling. Either RCP- or α5-RNAi or expression of $RCP^{379-649}$ blocked the ability of osteopontin to potentiate EGF-driven EGFR1 autophosphorylation and activation of PKB/Akt (Fig. 8 C). Collectively, these data indicate that after inhibition of αvβ3-mediated cell adhesion, EGFR1 was recruited into a physical complex with α5β1 and RCP, which enhances EGFR1 recycling to the plasma membrane and its ability to autophosphorylate and to signal via PKB/Akt.

Discussion

Fibroblasts and some tumor cells can move upon plastic or glass substrates in different ways (Pankov et al., 2005). Cells can migrate with persistence, allowing their translocation for considerable distances from the starting point. Alternatively, some

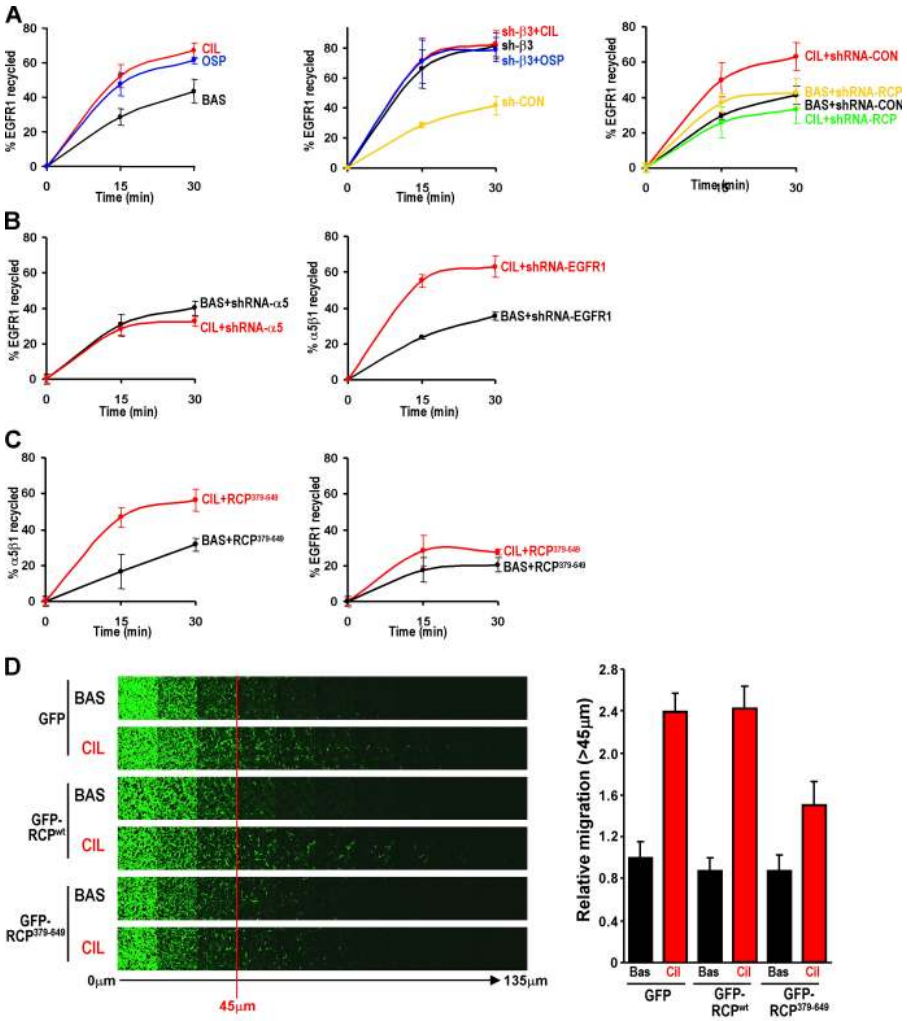

Figure 7. **α5β1 is required for recycling of EGFR1; and uncoupling EGFR1 recycling from α5β1 inhibits migration in 3D.** (A–C) Cells were transfected with short hairpin vectors targeting β3, α5, β1, RCP, or EGFR1 or with truncated GFP-RCP$^{379\text{-}649}$ as indicated. The receptor recycling protocol was then followed as for Fig. 1 A but with biotinylated EGFR1 or α5β1 integrin being determined by capture ELISA using microtitre wells coated with anti-EGFR1 or α5 integrin monoclonal antibodies as indicated by the y-axis labeling of the graphs. The proportion of EGFR1 or integrin recycled to the plasma membrane is expressed as a percentage of the pool of integrin labeled during the internalization period. Values are mean ± SEM; *n* = 3 or 4 independent experiments. (D) Migration of A2780 cells expressing GFP, GFP-RCP^{wt}, or GFP-RCP$^{379\text{-}649}$ into matrigel plugs containing 25 μg/ml FN. 1 μM cilengitide (CIL) was added as indicated to the matrigel and to both the upper and lower chambers of the inverted invasion assay. Migrating cells were detected and quantified as for Fig. 4. Values are mean ± SEM for three independent experiments.

cells move rapidly but with low persistence, thus remaining nearer their starting point. Previous analyses have shown that persistent migration occurs on FN substrates when αvβ3 is the dominant integrin, but when α5β1 dominates cells move more rapidly but with reduced persistence (Danen et al., 2005). We have shown that alterations in the relative rates at which αvβ3 and α5β1 traffic through the endosomal pathway can switch between slow/persistent and rapid/random migration in fibroblasts (White et al., 2007). When αvβ3 is cycling rapidly and is competent to engage ligand, the recycling of α5β1 is slow and cells migrate persistently. Alternatively, when αvβ3 trafficking is disrupted, α5β1 recycling is increased and this reduces migrational persistence. Here, we report that treatment of tumor cells with endogenous (soluble osteopontin) and pharmacological (cilengitide and c-RGDfV) antagonists of αvβ3 increases the rate at which α5β1 is transported from endosomes to the plasma membrane. This increased recycling requires the association of RCP with α5β1 and thus this Rab11 effector represents a key component of an integrin cross talk system that controls a switch between αvβ3- and α5β1-mediated migrational modes. Remarkably, we find that although α5β1-driven migration has little persistence on plastic or glass surfaces (2D), it corresponds to increased migration into a FN-rich 3D gel. Moreover, this type of cell movement was characterized by the extension of long pseudopods at the cell front as cells migrate on a 3D matrix, and RCP was concentrated at the tips of these invasive structures. This implies that α5β1 functions to promote tumor cell invasion and metastasis in vivo, with αvβ3 acting to restrain this.

The role of integrin recycling in this switching between αvβ3- and α5β1-mediated migration suggested that the recycling process itself was affecting integrin function. Although differences in the total levels of surface integrin could not explain the differences, it was possible that integrins required recycling to reactivate or to remove bound ligand fragments (Caswell and Norman, 2006). To test this hypothesis, we have measured the effect of cilengitide-induced recycling of α5β1 integrin (and its inhibition by dominant-negative RCP) on α5β1 surface expression and its ability to form adhesive bonds with substrate FN. The formation and the strength of the adhesive bonds was affected only to the extent expected for the contributions of αvβ3 and the small reduction of surface α5β1 levels caused by inhibition of recycling. Unlike the common static adhesion assays, this assay measures the force required for cell

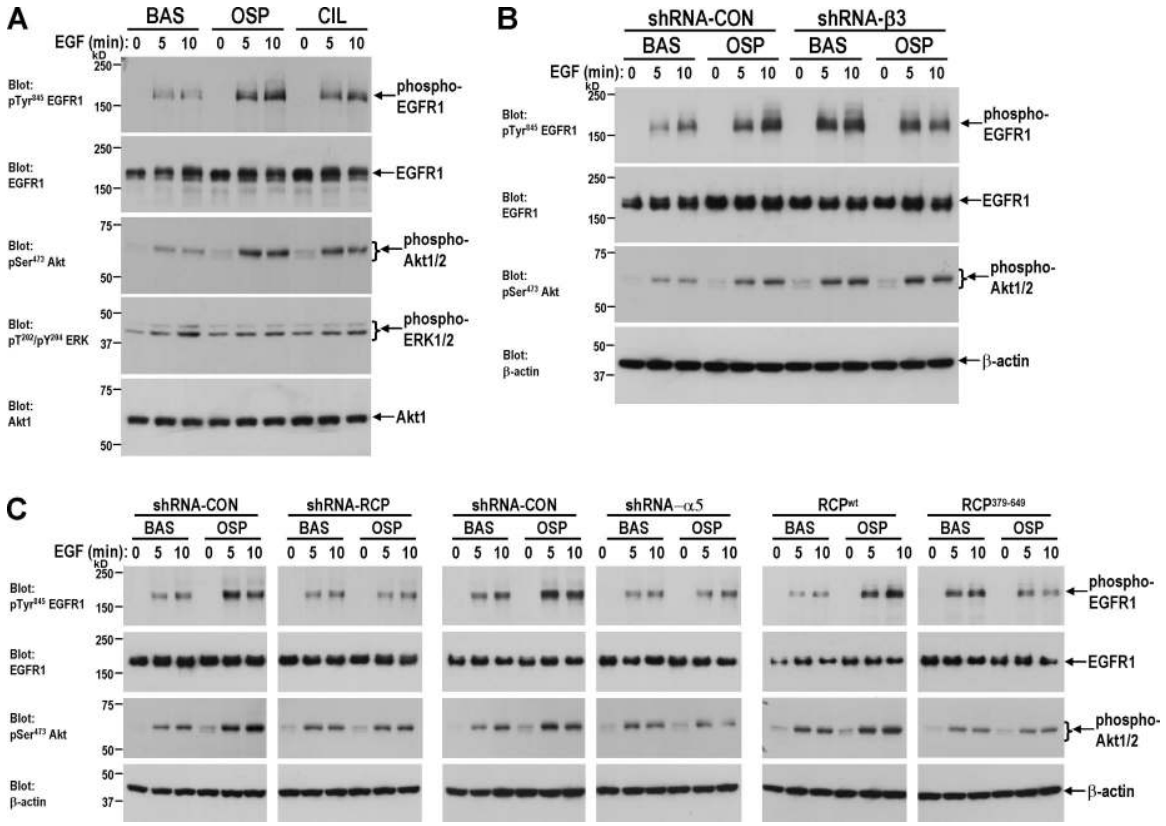

Figure 8. **Osteopontin enhances EGFR1 signaling via a mechanism that requires α5β1, RCP, and association of EGFR1 with RCP.** Cells were transfected with short hairpin vectors targeting β3, α5, β1, RCP or EGFR1 or with truncated GFP-RCP$^{379\text{-}649}$ as indicated. Cells were serum starved overnight followed by a 40-min treatment with either 1 μM cilengitide or 0.5 μg/ml osteopontin. The cells were then challenged with EGF for the indicated times and lysed. Levels of active phosphoTyr^{845}-EGFR1, phosphoSer^{473}-Akt, and phosphoThr^{202}/phosphoTyr^{204}-ERK were determined by Western blotting. Protein loading of β-actin, Akt1, and EGFR1 was confirmed by Western blotting.

detachment, which is directly proportional to the number of adhesive integrin bonds (Shi and Boettiger, 2003; Boettiger, 2007). Therefore, recycling had no effect on ligand binding and adhesive function of α5β1 integrin.

The absence of an effect of trafficking on integrin adhesive function led us to examine the influence of α5β1 recycling on cell signaling. Studies on tumor angiogenesis in mice show clearly that knockout of β3 leads to increased endothelial cell proliferation and migration owing to increased VEGFR2 signaling (Reynolds et al., 2004). Other studies have described physical complexes formed by integrins and RTKs, but the way in which these associations may regulate signaling is not clear (Schneller et al., 1997; Soldi et al., 1999). Here we have found that RCP is required to bring α5β1 and EGFR1 together into a physical complex and, although our results do not resolve all of the details of the RCP–α5β1–EGFR1 complex (such as whether these associations involve direct molecular contacts between α5β1 and RCP and EGFR1 and RCP, respectively), we have determined how the trafficking of EGFR1 is coordinated with α5β1. Clearly knockdown of α5β1 opposes the coprecipitation of RCP with EGFR1, indicating that recruitment of RCP's C-terminal region to α5β1 may likely be a prerequisite for subsequent association of the N terminus of RCP with EGFR1 and for subsequent enhanced EGFR1 recycling. In this regard, it is possible that α5β1 is acting as a "receptor" for RCP to guide this Rab effector to a membrane subdomain, whereupon a secondary association with EGFR1 is formed.

Efficient signaling from EGFR1 to the Ras–MEK–ERK axis requires receptor internalization, and a close association between EGFR1 and components of the MAPK cascade has been observed to occur at late endosomes (von Zastrow and Sorkin, 2007). Conversely, it appears that EGFR1-stimulated activation of phosphoinositide-3 kinase most likely occurs at or near the plasma membrane and that communication between EGFR1 and PKB/Akt is terminated after receptor endocytosis (Haugh and Meyer, 2002). In view of this, we propose that RCP-dependent recycling acts to slow the rate at which EGFR1 reaches later endosomes where sustained activation of MAPKs occurs and favors its localization to the plasma membrane or recycling compartments where the receptor can recruit phosphoinositide-3 kinase and thereby activate PKB/Akt. Indeed a recent study has found that c-Src promotes the trafficking of FGF receptor from endosomes to the plasma membrane and that this favors activation of PKB/Akt over signaling to the MEK–ERK axis (Sandilands et al., 2007). We find that c-Src binds to RCP and that this kinase is required for integrin and RTK recycling (unpublished data). Osteopontin enhances EGFR1 signaling in a way that involves c-Src (Das et al., 2004), which in light of the data presented here is likely to be mediated by RCP-dependent effects on α5β1 and EGFR1 trafficking. Furthermore,

we find that RTK recycling and signaling is influenced by RCP/α5β1 in other cell types, including VEGFR2 in endothelial cells and FGF receptor in fibroblasts (unpublished data). It is interesting to note that the genes for RCP and FGF receptor 1 are located close to one another within the 8p11-12 chromosomal region that is amplified in several cancers, including some breast tumors (Gelsi-Boyer et al., 2005). In this regard, it will be necessary to determine the molecular details of this apparently promiscuous association of RTKs with the RCP–α5β1 complex and how this influences their trafficking and signaling in cancer types where the 8p11-12 chromosomal locus is amplified.

In phase I and II clinical trails cilengitide has elicited some enduring responses in glioma patients (Nabors et al., 2007), but the results for other types of cancer are not encouraging (Friess et al., 2006; Hariharan et al., 2007). Indeed, the role that αvβ3 plays in cancer-relevant processes is controversial, as some studies implicate αvβ3 as a proangiogenic integrin (Brooks et al., 1994), whereas other work contradicts this (Reynolds et al., 2002). Our findings support both pro- and antiinvasive roles for αvβ3, as knockdown of αvβ3 can reduce A2780 cell migration but only in the absence of FN or when RCP-dependent processes are compromised. Conversely, when FN is abundant and α5β1 and RCP are present (as is the case in many tumor types), inhibition of αvβ3 strongly promotes tumor cell migration, thus overriding the capacity for this integrin to function as an antimigratory molecule. We consistently find that cellular responses to cilengitide, c-RGDfV, small molecule inhibitors of αvβ3 (unpublished data), and osteopontin are indistinguishable from one another (and from β3 knockdown), indicating the possibility that the lack of efficacy of anti-αvβ3 compounds in cancer may be owing to the capacity of these molecules to mimic the prometastatic effects of osteopontin.

In conclusion, our surprising finding that inhibition of αvβ3 leads to increased tumor cell migration in 3D microenvironments, and the elucidation of the RCP–α5β1–EGFR1–dependent mechanisms that drive this, highlight the need to fully understand how integrin trafficking regulates cell migration if the therapeutic potential of anti-integrin agents is to be maximized.

Materials and methods

Cell culture and transfection
A2780 cells were maintained in RPMI supplemented with 10% (vol/vol) serum at 37°C and 10% CO_2. All constructs, shRNAi vectors, and RNAi oligonucleotides were transfected into cells using the Nucleofector system (solution T, program A-23; Amaxa) according to the manufacturer's instructions. All plasmids were purified by CsCl banding before transfection by nucleofection.

Plasmid constructs
The Rab11-FIP constructs have been previously described as follows: pEGFP-C3 RCP and pEGFP-C1 $RCP^{379\text{-}649}$ in Damiani et al. (2004); pEGFP-C1 FIP2 in Lindsay and McCaffrey (2002); pEGFP-C1 Rip11, pEGFP-C1 $Rip11^{630E}$, pEGFP-C3 RCP^{621E}, and pEGFP-C1 $FIP2^{481E}$ in Lindsay and McCaffrey (2004b).

Immunoprecipitation and Western blotting
A2780 cells were lysed in lysis buffer (200 mM NaCl, 75 mM Tris-HCl, pH 7, 15 mM NaF, 1.5 mM Na_3VO_4, 7.5 mM EDTA, 7.5 mM EGTA, 0.15% (vol/vol) Tween-20, 50 µg/ml leupeptin, 50 µg/ml aprotinin, and 1 mM 4-(2-aminoethyl)-benzenesulfonyl fluoride). Lysates were passed three times through a 27-gauge needle and clarified by centrifugation at 10,000 *g* for 10 min at 4°C. Magnetic beads conjugated to sheep anti–mouse IgG (Invitrogen) were bound to anti-integrin (anti-α5 or anti-β3; BD Biosciences), anti-GFP (Abcam), or control monoclonal (RG-16; Sigma-Aldrich) antibodies. Antibody-coated beads were incubated with lysates for 2 h at 4°C with constant rotation. Unbound proteins were removed by extensive washing in lysis buffer, and specifically associated proteins were eluted from the beads by boiling for 10 min in Laemmli sample buffer. Proteins were resolved by SDS-PAGE and analyzed by Western blotting as described previously (Roberts et al., 2001). Antibodies used for Western blotting were as follows: anti-α5 integrin (BD Biosciences), anti-β1 integrin (BD Biosciences), anti-β3 integrin (BD Biosciences; blots using this antibody were run under nonreducing conditions), anti-RCP (Genway), anti-EGFR1 (BD Biosciences) and anti-GFP (Abcam).

Inverted matrigel plug assay
Inverted matrigel assays were performed as described previously (Hennigan et al., 1994). In brief, matrigel supplemented with 25 µg/ml FN as indicated was allowed to polymerize in transwell inserts (Corning) for 1 h at 37°C. Inserts were then inverted and cells were seeded directly onto the opposite face of the filter. Transwell inserts were finally placed in serum-free medium, and medium supplemented with 10% FCS and 30 ng/ml EGF was placed on top of the matrix, providing a chemotactic gradient. Where appropriate, 1 µM cilengitide, 0.5 µg/ml osteopontin, and 1.0 µg/ml of integrin/FN-blocking antibodies were added to the matrigel before plug polymerization and also to the medium throughout the system. 48 h after seeding, migrating cells were stained with Calcein AM and visualized by confocal microscopy with serial optical sections being captured at 15-µm intervals.

Generation of cell-derived matrix
Cell-derived matrix was generated as described previously (Cukierman et al., 2001; Bass et al., 2007). In brief, gelatin-coated tissue culture-ware was cross-linked with glutaraldehyde, quenched, and equilibrated in DME containing 10% FCS. Primary cultured human dermal fibroblasts were seeded at near confluence ($\sim 2 \times 10^4$ cells/cm^2) and grown for 10 d in DME containing 10% FCS and 50 µg/ml ascorbic acid. Matrices were denuded of living cells by incubation with PBS containing 20 mM NH_4OH and 0.5% Triton X-100, and DNA residue was removed by incubation with DNaseI. Matrices were blocked with 0.1% heat-denatured BSA before seeding of cells.

Receptor internalization and recycling assays
Internalization and recycling assays were performed after 30–45 min of serum starvation and subsequently conducted, including the internalization and recycling periods, in the absence of serum. Integrin and EGFR1 internalization and recycling assays were performed as described previously (Roberts et al., 2001). Internalization assays were performed in the presence of 0.6 mM of primaquine as described in Roberts et al. (2001). For measurement of recycling, the receptor internalization conditions were 30 min at 37°C for all experiments. The antibodies used for capture ELISA detection of α5β1 integrin and EGFR1 were obtained from BD Biosciences. Cilengitide, osteopontin, cRADfV, and cRGDfV were added to the cells only during the recycling period.

^{125}I-labeled transferrin recycling assays were performed essentially as described in van Dam and Stoorvogel (2002) with some modifications. In brief, serum-starved cells were incubated with ^{125}I-labeled transferrin (0.1 µCi/well; PerkinElmer) for 1 h at 4°C in PBS with 1% (wt/vol) BSA. The tracer was allowed to internalize for 30 min at 37°C (to label the recycling compartment). Tracer remaining at the cell surface was removed by incubation with acid PBS (corrected to pH 4.0 by the addition of HCl) at 4°C for 6 min, and the tracer was allowed to recycle at 37°C in serum-free DME supplemented with 1% BSA and 50 µM desferoxamine (Sigma-Aldrich). The quantity of ^{125}I recycled into the medium is expressed as a percentage of the number of counts incorporated during the internalization period.

Microscopy, track-plot analysis, and 3D reconstruction
Confluent monolayers were wounded with a plastic pipette tip and placed on the stage of an inverted microscope (Axiovert S100; Carl Zeiss, Inc.) in an atmosphere of 5% CO_2 at 37°C. Cells were observed using a 20× phase-contrast objective and images were collected every 20 min using a digital camera (C4742-95; Hamamatsu Photonics). Movies were generated and cell tracks were analyzed using Bioimaging software (Andor). For fluorescence time-lapse imaging, cells were plated onto 6-well plates or glass-bottomed 3-cm plates (coated with cell-derived matrix as appropriate)

and incubated at 37°C until cells adhered and began migrating (4 h). Cells were imaged using a 10× objective and an inverted microscope in an atmosphere of 5% CO_2 at 37°C or a 64× objective and an inverted confocal microscope (Fluoview FV1000; Olympus) in an atmosphere of 5% CO_2 at 37°C. For immunofluorescence, cell were fixed in 4% paraformaldehyde for 10 min and then permeabilized in PBS containing 0.2% Triton X-100. Primary antibodies for immunofluorescence were α5 integrin (BD Biosciences), RCP (Genway), and EGFR1 (BD Biosciences) with F-actin being detected using $BODIPY_{650/665}$-phalloidin (Invitrogen). Immunofluorescence was imaged using a 64× objective and an inverted confocal microscope. Images from the confocal microscope were imported into Photoshop (Adobe) and linear-only adjustments made to their brightness and contrast.

To generate 3D reconstructions, serial z-stack images were captured using a 64× objective and an inverted confocal microscope and imported into Volocity Visualization (Improvision). Individual cells were cropped in the XY plane from fields of view containing more than one cell. HR opacity rendering was used to create a 3D image, which was rotated along the x axis to create XZ, XZ, and XYZ projections.

Assessment of EGF signaling

Cells were serum starved overnight. On the day of the experiment, cells were treated with either 1 µM cilengitide or 0.5 µg/ml osteopontin for 40 min, immediately before a challenge with 30 ng/ml EGF (Sigma-Aldrich) for 5 or 10 min as indicated. Western blotting was then used to determine levels of active signaling moieties using the following antibodies: anti–phosphoTyr^{845}–EGFR1 (Cell Signaling Technology), anti–phosphoSer^{473}–Akt (Cell Signaling Technology), and anti–phosphoThr^{202}/phosphoTyr^{204}–ERK (Cell Signaling Technology). The following antibodies were used to assess protein loading: anti-EGFR1 (BD Biosciences), anti-Akt1 (Cell Signaling Technology), and β-actin (Sigma-Aldrich).

Spinning disc methods

A2780 cells transfected with RCP^{wt} or RCP^{621E} were plated overnight in complete medium ± 1 µM cilengitide for the last 16 h. Cells were dissociated with 2 mM EDTA and single cell suspensions were added to FN-coated (5 µg/ml) glass coverslips and incubated at 25°C for 60 min. Coverslips were placed on the spinning disc device and exposed to a linear hydrodynamic shear gradient for 5 min (Boettiger, 2007). Coverslips were removed from the spinning device, fixed in formalin, permeabilized, and stained with DAPI. 61 fields at 15 different radial positions plus the center were counted for 1-µm-diameter fields and plotted as a function of shear stress. Curve fits were performed using SigmaPlot 7.0 using the formula $f = 1/\{a - \exp[b\ (t - c)]\}$, where f is the fraction of adherent cells, t is the corresponding shear stress, and a, b, and c are fit parameters; c is the shear stress for 50% detachment.

Online supplemental material

Fig. S1 A displays Western blots indicating the efficacy of shRNA vectors targeting β3 and α5 integrins, EGFR1, and RCP. Fig. S1 B shows results from internalization assays indicating that addition of cilengitide and expression of dominant-negative RCP^{621E} do not greatly influence the constitutive endocytosis of α5β1 or EGFR1. Fig. S2 indicates the inability of dominant-negative $Rab11^{124I}$, $Rip11^{630E}$, $FIP2^{480E}$, and RCP^{621E} to influence recycling of α5β1 integrin and Tfn-R. Fig. S3 shows the time course over which physical association of GFP-RCP and α5β1 integrin is established after the addition of cilengitide and shows the lack of coprecipitation of paxillin with GFP-RCP. Fig. S4 shows confocal immunofluorescence images illustrating the influence of cilengitide/osteopontin or knockdown of β3 integrin on cellular morphology and the distribution of α5β1 and RCP. Fig. S5 shows data indicating that dominant-negative $Rip11^{630E}$ and $FIP2^{480E}$ do not influence migration through FN-containing matrigel, and Fig. S5 B documents the consequences of expression of dominant-negative RCP^{621E} and/or addition of cilengitide on α5β1 and EGFR1 surface expression. Videos 1–3 show that addition of cilengitide promotes a rapid/random mode of cell migration on 2D surfaces that is opposed by expression of dominant-negative RCP^{621E}. Videos 4–6 show that whereas A2780 cells expressing GFP-actin extend an organized fan-like lamellipodium as they move, after treatment with cilengitide or osteopontin their movement is characterized by the formation of highly dynamic actin-rich protrusions at the cell front. Videos 7–9 show that cilengitide promotes a pseudopodial mode of cell migration on cell-derived matrix that is opposed by expression of RCP^{621E}. Video 10 is a high-resolution fluorescence time-lapse sequence showing GFP-RCP localization to the tip of the extending pseudopod as A2780 cells migrate on a 3D matrix. Online supplemental material is available at http://www.jcb.org/cgi/content/full/jcb.200804140/DC1.

J.C. Norman and P.T. Caswell are supported by Cancer Research UK. M.W. McCaffrey is supported by a Science Foundation Ireland investigator grant (05/IN.3/B 859). M. Chan and D. Boettiger are supported by grant RO1 GM 53788 (Institute of General Medicine, National Institutes of Health).

Submitted: 24 April 2008
Accepted: 4 September 2008

References

Bass, M.D., K.A. Roach, M.R. Morgan, Z. Mostafavi-Pour, T. Schoen, T. Muramatsu, U. Mayer, C. Ballestrem, J.P. Spatz, and M.J. Humphries. 2007. Syndecan-4–dependent Rac1 regulation determines directional migration in response to the extracellular matrix. *J. Cell Biol.* 177:527–538.

Boettiger, D. 2007. Quantitative measurements of integrin-mediated adhesion to extracellular matrix. *Methods Enzymol.* 426:1–25.

Boettiger, D., F. Huber, L. Lynch, and S. Blystone. 2001. Activation of alpha(v)beta3-vitronectin binding is a multistage process in which increases in bond strength are dependent on Y747 and Y759 in the cytoplasmic domain of beta3. *Mol. Biol. Cell.* 12:1227–1237.

Brooks, P.C., R.A. Clark, and D.A. Cheresh. 1994. Requirement of vascular integrin alpha v beta 3 for angiogenesis. *Science.* 264:569–571.

Caswell, P.T., and J.C. Norman. 2006. Integrin trafficking and the control of cell migration. *Traffic.* 7:14–21.

Caswell, P.T., H.J. Spence, M. Parsons, D.P. White, K. Clark, K.W. Cheng, G.B. Mills, M.J. Humphries, A.J. Messent, K.I. Anderson, et al. 2007. Rab25 associates with alpha5beta1 integrin to promote invasive migration in 3D microenvironments. *Dev. Cell.* 13:496–510.

Cheng, K.W., J.P. Lahad, W.L. Kuo, A. Lapuk, K. Yamada, N. Auersperg, J. Liu, K. Smith-McCune, K.H. Lu, D. Fishman, et al. 2004. The RAB25 small GTPase determines aggressiveness of ovarian and breast cancers. *Nat. Med.* 10:1251–1256.

Cukierman, E., R. Pankov, D.R. Stevens, and K.M. Yamada. 2001. Taking cell-matrix adhesions to the third dimension. *Science.* 294:1708–1712.

Damiani, M.T., M. Pavarotti, N. Leiva, A.J. Lindsay, M.W. McCaffrey, and M.I. Colombo. 2004. Rab coupling protein associates with phagosomes and regulates recycling from the phagosomal compartment. *Traffic.* 5:785–797.

Danen, E.H., J. van Rheenen, W. Franken, S. Huveneers, P. Sonneveld, K. Jalink, and A. Sonnenberg. 2005. Integrins control motile strategy through a Rho–cofilin pathway. *J. Cell Biol.* 169:515–526.

Das, R., G.H. Mahabeleshwar, and G.C. Kundu. 2004. Osteopontin induces AP-1-mediated secretion of urokinase-type plasminogen activator through c-Src-dependent epidermal growth factor receptor transactivation in breast cancer cells. *J. Biol. Chem.* 279:11051–11064.

Dechantsreiter, M.A., E. Planker, B. Matha, E. Lohof, G. Holzemann, A. Jonczyk, S.L. Goodman, and H. Kessler. 1999. N-Methylated cyclic RGD peptides as highly active and selective alpha(V)beta(3) integrin antagonists. *J. Med. Chem.* 42:3033–3040.

Fan, G.H., L.A. Lapierre, J.R. Goldenring, J. Sai, and A. Richmond. 2004. Rab11-family interacting protein 2 and myosin Vb are required for CXCR2 recycling and receptor-mediated chemotaxis. *Mol. Biol. Cell.* 15:2456–2469.

Friess, H., J.M. Langrehr, H. Oettle, J. Raedle, M. Niedergethmann, C. Dittrich, D.K. Hossfeld, H. Stoger, B. Neyns, P. Herzog, et al. 2006. A randomized multi-center phase II trial of the angiogenesis inhibitor Cilengitide (EMD 121974) and gemcitabine compared with gemcitabine alone in advanced unresectable pancreatic cancer. *BMC Cancer.* 6:285.

Garcia, A.J., F. Huber, and D. Boettiger. 1998. Force required to break alpha-5beta1 integrin-fibronectin bonds in intact adherent cells is sensitive to integrin activation state. *J. Biol. Chem.* 273:10988–10993.

Gelsi-Boyer, V., B. Orsetti, N. Cervera, P. Finetti, F. Sircoulomb, C. Rouge, L. Lasorsa, A. Letessier, C. Ginestier, F. Monville, et al. 2005. Comprehensive profiling of 8p11-12 amplification in breast cancer. *Mol. Cancer Res.* 3:655–667.

Goldenring, J.R., G.S. Ray, and J.R. Lee. 1999. Rab11 in dysplasia of Barrett's epithelia. *Yale J. Biol. Med.* 72:113–120.

Hales, C.M., R. Griner, K.C. Hobdy-Henderson, M.C. Dorn, D. Hardy, R. Kumar, J. Navarre, E.K. Chan, L.A. Lapierre, and J.R. Goldenring. 2001. Identification and characterization of a family of Rab11-interacting proteins. *J. Biol. Chem.* 276:39067–39075.

Hariharan, S., D. Gustafson, S. Holden, D. McConkey, D. Davis, M. Morrow, M. Basche, L. Gore, C. Zang, C.L. O'Bryant, et al. 2007. Assessment of the biological and pharmacological effects of the alpha nu beta3 and alpha nu beta5 integrin receptor antagonist, cilengitide (EMD 121974), in patients with advanced solid tumors. *Ann. Oncol.* 18:1400–1407.

Haugh, J.M., and T. Meyer. 2002. Active EGF receptors have limited access to PtdIns(4,5)P(2) in endosomes: implications for phospholipase C and PI 3-kinase signaling. *J. Cell Sci.* 115:303–310.

Hennigan, R.F., K.L. Hawker, and B.W. Ozanne. 1994. Fos-transformation activates genes associated with invasion. *Oncogene.* 9:3591–3600.

Hickson, G.R., J. Matheson, B. Riggs, V.H. Maier, A.B. Fielding, R. Prekeris, W. Sullivan, F.A. Barr, and G.W. Gould. 2003. Arfophilins are dual Arf/Rab 11 binding proteins that regulate recycling endosome distribution and are related to *Drosophila* nuclear fallout. *Mol. Biol. Cell.* 14:2908–2920.

Horgan, C.P., M. Walsh, T.H. Zurawski, and M.W. McCaffrey. 2004. Rab11-FIP3 localises to a Rab11-positive pericentrosomal compartment during interphase and to the cleavage furrow during cytokinesis. *Biochem. Biophys. Res. Commun.* 319:83–94.

Horgan, C.P., A. Oleksy, A.V. Zhdanov, P.Y. Lall, I.J. White, A.R. Khan, C.E. Futter, J.G. McCaffrey, and M.W. McCaffrey. 2007. Rab11-FIP3 is critical for the structural integrity of the endosomal recycling compartment. *Traffic.* 8:414–430.

Hynes, R.O. 2002. Integrins: bidirectional, allosteric signaling machines. *Cell.* 110:673–687.

Jones, M.C., P.T. Caswell, and J.C. Norman. 2006. Endocytic recycling pathways: emerging regulators of cell migration. *Curr. Opin. Cell Biol.* 18:549–557.

Khodavirdi, A.C., Z. Song, S. Yang, C. Zhong, S. Wang, H. Wu, C. Pritchard, P.S. Nelson, and P. Roy-Burman. 2006. Increased expression of osteopontin contributes to the progression of prostate cancer. *Cancer Res.* 66:883–888.

Lindsay, A.J., and M.W. McCaffrey. 2002. Rab11-FIP2 functions in transferrin recycling and associates with endosomal membranes via its COOH-terminal domain. *J. Biol. Chem.* 277:27193–27199.

Lindsay, A.J., and M.W. McCaffrey. 2004a. The C2 domains of the class I Rab11 family of interacting proteins target recycling vesicles to the plasma membrane. *J. Cell Sci.* 117:4365–4375.

Lindsay, A.J., and M.W. McCaffrey. 2004b. Characterisation of the Rab binding properties of Rab coupling protein (RCP) by site-directed mutagenesis. *FEBS Lett.* 571:86–92.

Lindsay, A.J., A.G. Hendrick, G. Cantalupo, F. Senic-Matuglia, B. Goud, C. Bucci, and M.W. McCaffrey. 2002. Rab coupling protein (RCP), a novel Rab4 and Rab11 effector protein. *J. Biol. Chem.* 277:12190–12199.

Nabors, L.B., T. Mikkelsen, S.S. Rosenfeld, F. Hochberg, N.S. Akella, J.D. Fisher, G.A. Cloud, Y. Zhang, K. Carson, S.M. Wittemer, et al. 2007. Phase I and correlative biology study of cilengitide in patients with recurrent malignant glioma. *J. Clin. Oncol.* 25:1651–1657.

Pankov, R., Y. Endo, S. Even-Ram, M. Araki, K. Clark, E. Cukierman, K. Matsumoto, and K.M. Yamada. 2005. A Rac switch regulates random versus directionally persistent cell migration. *J. Cell Biol.* 170:793–802.

Peden, A.A., E. Schonteich, J. Chun, J.R. Junutula, R.H. Scheller, and R. Prekeris. 2004. The RCP-Rab11 complex regulates endocytic protein sorting. *Mol. Biol. Cell.* 15:3530–3541.

Pellinen, T., and J. Ivaska. 2006. Integrin traffic. *J. Cell Sci.* 119:3723–3731.

Prekeris, R. 2003. Rabs, Rips, FIPs, and endocytic membrane traffic. *ScientificWorldJournal.* 3:870–880.

Rangaswami, H., A. Bulbule, and G.C. Kundu. 2006. Osteopontin: role in cell signaling and cancer progression. *Trends Cell Biol.* 16:79–87.

Reynolds, L.E., L. Wyder, J.C. Lively, D. Taverna, S.D. Robinson, X. Huang, D. Sheppard, R.O. Hynes, and K.M. Hodivala-Dilke. 2002. Enhanced pathological angiogenesis in mice lacking beta3 integrin or beta3 and beta5 integrins. *Nat. Med.* 8:27–34.

Reynolds, A.R., L.E. Reynolds, T.E. Nagel, J.C. Lively, S.D. Robinson, D.J. Hicklin, S.C. Bodary, and K.M. Hodivala-Dilke. 2004. Elevated Flk1 (vascular endothelial growth factor receptor 2) signaling mediates enhanced angiogenesis in beta3-integrin-deficient mice. *Cancer Res.* 64:8643–8650.

Rittling, S.R., and A.F. Chambers. 2004. Role of osteopontin in tumour progression. *Br. J. Cancer.* 90:1877–1881.

Rittling, S.R., Y. Chen, F. Feng, and Y. Wu. 2002. Tumor-derived osteopontin is soluble, not matrix associated. *J. Biol. Chem.* 277:9175–9182.

Roberts, M., S. Barry, A. Woods, P. van der Sluijs, and J. Norman. 2001. PDGF-regulated rab4-dependent recycling of alphavbeta3 integrin from early endosomes is necessary for cell adhesion and spreading. *Curr. Biol.* 11:1392–1402.

Sahai, E. 2005. Mechanisms of cancer cell invasion. *Curr. Opin. Genet. Dev.* 15:87–96.

Sandilands, E., S. Akbarzadeh, A. Vecchione, D.G. McEwan, M.C. Frame, and J.K. Heath. 2007. Src kinase modulates the activation, transport and signalling dynamics of fibroblast growth factor receptors. *EMBO Rep.* 8:1162–1169.

Schneller, M., K. Vuori, and E. Ruoslahti. 1997. Alphavbeta3 integrin associates with activated insulin and PDGFbeta receptors and potentiates the biological activity of PDGF. *EMBO J.* 16:5600–5607.

Shi, Q., and D. Boettiger. 2003. A novel mode for integrin-mediated signaling: tethering is required for phosphorylation of FAK Y397. *Mol. Biol. Cell.* 14:4306–4315.

Soldi, R., S. Mitola, M. Strasly, P. Defilippi, G. Tarone, and F. Bussolino. 1999. Role of alphavbeta3 integrin in the activation of vascular endothelial growth factor receptor-2. *EMBO J.* 18:882–892.

Spence, H.J., L. McGarry, C.S. Chew, N.O. Carragher, L.A. Scott-Carragher, Z. Yuan, D.R. Croft, M.F. Olson, M. Frame, and B.W. Ozanne. 2006. AP-1 differentially expressed proteins Krp1 and fibronectin cooperatively enhance Rho-ROCK-independent mesenchymal invasion by altering the function, localization, and activity of nondifferentially expressed proteins. *Mol. Cell. Biol.* 26:1480–1495.

Tuck, A.B., D.M. Arsenault, F.P. O'Malley, C. Hota, M.C. Ling, S.M. Wilson, and A.F. Chambers. 1999. Osteopontin induces increased invasiveness and plasminogen activator expression of human mammary epithelial cells. *Oncogene.* 18:4237–4246.

Tuck, A.B., C. Hota, S.M. Wilson, and A.F. Chambers. 2003. Osteopontin-induced migration of human mammary epithelial cells involves activation of EGF receptor and multiple signal transduction pathways. *Oncogene.* 22:1198–1205.

van Dam, E.M., and W. Stoorvogel. 2002. Dynamin-dependent transferrin receptor recycling by endosome-derived clathrin-coated vesicles. *Mol. Biol. Cell.* 13:169–182.

von Zastrow, M., and A. Sorkin. 2007. Signaling on the endocytic pathway. *Curr. Opin. Cell Biol.* 19:436–445.

Wallace, D.M., A.J. Lindsay, A.G. Hendrick, and M.W. McCaffrey. 2002. Rab11-FIP4 interacts with Rab11 in a GTP-dependent manner and its overexpression condenses the Rab11 positive compartment in HeLa cells. *Biochem. Biophys. Res. Commun.* 299:770–779.

White, D.P., P.T. Caswell, and J.C. Norman. 2007. αvβ3 and α5β1 integrin recycling pathways dictate downstream Rho kinase signaling to regulate persistent cell migration. *J. Cell Biol.* 177:515–525.

Yoon, S.O., S. Shin, and A.M. Mercurio. 2005. Hypoxia stimulates carcinoma invasion by stabilizing microtubules and promoting the Rab11 trafficking of the alpha6beta4 integrin. *Cancer Res.* 65:2761–2769.